Leak Monitoring

Ramon Pérez, Josep Cugueró, Gerard Sanz, Miquel A. Cugueró, Joaquim Blesa

Abstract The efficient use of water resources is a subject of major concern for water utilities and authorities. One of the main challenges in improving the efficiency of drinking water networks is to minimize water loss in pipes due to leakage. Water leaks in water distribution networks are unavoidable. They can cause significant economic losses in fluid transportation and an increase on reparation costs that finally generate an extra cost for the final consumer due to the waste of energy and chemicals in water treatment plants. Besides, leaks may also damage infrastructure and cause third party damage and health risks. The loss of about 15 % of treated water in developed countries and 35 % in developing countries is a rather critical issue in a world struggling to satisfy water demands of a growing population [2]. This chapter presents the state of the art of the leak management including the real-time monitoring that allows the leak detection and localization, techniques for repair and minimization based on the system control. Special attention will be given to model-based approaches. The deep description of a leak location method based on sensitivity matrix and the correlation analysis will be provided in this Chapter with the application to a real case study.

Ramon Pérez Magrané
Polytechnic University of Catalonia, Terrassa 08222, Spain. e-mail: ramon.perez@upc.edu

Josep Cugueró
Polytechnic University of Catalonia, Terrassa 08222, Spain. e-mail: josep.cuguero@upc.edu

Gerard Sanz Estapé
Polytechnic University of Catalonia, Terrassa 08222, Spain. e-mail: gerard.sanz@upc.edu

Miquel A. Cugueró
Polytechnic University of Catalonia, Terrassa 08222, Spain. e-mail: miquel.angel.cuguero@upc.edu

Joaquim Blesa
Institut de Robòtica i Informàtica Industrial, CSIC-UPC, Barcelona 08028, Spain. e-mail: jblesa@iri.upc.edu

1 Introduction

Waste and loss of water have been sometimes disregarded due to the low water price and ease of exploitation in developed countries. However, both users and utilities are increasing their concern to avoid present and future water scarcity. Individual users can optimise their daily routines to reduce water waste, but burst and background leakage will be present independently of it.

Leakage in water distribution systems has attracted a lot of attention by both practitioners and researchers over the past years. Leak identification is divided into leakage awareness and leak localization, as suggested in the review of leakage management related methods in distribution pipe systems from detection and assessment to efficient control [22]. Leakage awareness focuses on leak detection in the network, but does not give any information about its precise location [9, 13, 14, 15, 25]. On the other hand, leakage localization is an activity that identifies and prioritises the areas of leakage to make pinpointing of leaks easier [26]. Leak localization techniques can be divided into two categories: external and internal [1]. The use of external methods like acoustic logging [20], penetrating radar [8] or liquid detection methods [7] has some drawbacks like needing a large number of sensors, not being suitable for application in large urban areas, or being invasive. Internal methods use continuously monitored data to infer the position of leaks using models. Many techniques in literature are based on transient analysis, which is mainly used on single, grounded pipelines due to the high effect of the system uncertainty on results [11, 29, 10, 4]. Non-transient model-based leakage localization techniques have been also developed during the last years [18, 5, 6, 19]. These techniques analyse the difference between measurements and estimated values from leaky scenarios to signal the probability of a zone to contain leakage.

The use of models for monitoring and supervising water distribution networks (WDN) is a common practice in water companies. A good calibration of these models is required to obtain reliable results when using them [28], as it has been analysed in chapters 3, 4 and 5. Once the model is calibrated, the model-based leak detection and localization methodologies reviewed can make use of it. However, these methodologies do not consider the evolution of demands in the real system. This evolution should be taken into account because demands are parameters that change continuously and leakages may be masked with their evolution [27, 30].

2 Problem Statement

Given a model for the non-transient behaviour of a network and a sequence of measurements from it, the problem is to locate a node in the network where there may be a leak. Two kind of measurements can be distinguished: boundary conditions, which are pressure $\mathbf{h}^S$ and total inflow q^{in} at the n_h inputs of the network, and additional n_y head measurements $\mathbf{y} = (y_1 \dots y_{n_y})$ from selected nodes in the network. Measurements are acquired at sampling time T_s but, as the effect of a leak over the

measurements is usually small and has fluctuations due to sensor resolution, the localization methodology is applied at a larger time T_L. Thus, $N_L = T_L/T_s$ measurements are available between two consecutive iterations. Assuming that the boundary conditions have not changed significantly during T_L, the mean of the measurement y_i at instant kT_L ($\bar{y}_i(kT_L)$) is computed as

$$\bar{y}_i(kT_L) = \frac{\sum_{j=0}^{N_L-1} y_i(kT_L - jT_s)}{N_L} \tag{1}$$

For clarity, the time argument is only made explicit when necessary.

2.1 Model of the network

In the absence of leakage, the total inflow q^{in} is distributed among the network nodes according to a given demand pattern. The demands of the nodes are represented by a vector $\mathbf{d} = (d_1, \ldots d_{n_d})$ with n_d equal to the number of nodes in the network. In a non-leakage scenario the total inflow is equal to the sum of demands

$$q^{in} = \sum_{i=1}^{n_d} d_j \tag{2}$$

where each demand d_i can be related to q^{in} by a weight, i.e.

$$d_i(q^{in}) = \alpha_i q^{in} \tag{3}$$

Given the boundary conditions, the computation of a prediction $\hat{\mathbf{y}}_{\mathbf{nf}}$ for a non-leakage scenario is denoted by

$$\hat{\mathbf{y}}_{\mathbf{nf}} = \mathbf{g}_{nf}(q^{in}, \mathbf{h}_S, \mathbf{d}(q^{in})) \tag{4}$$

where $\hat{\mathbf{y}}_{\mathbf{nf}} \in \Re^{n_y}$, $\mathbf{g}_{nf} : \Re \times \Re^{n_h} \times \Re^{n_d} \rightarrow \Re^{n_y}$, $\mathbf{h}_S \in \Re^{n_h}$ and $\mathbf{d} \in \Re^{n_d}$. Subscript nf indicates non-faulty, i.e. non-leakage scenario. The difference

$$\mathbf{r} = \mathbf{y} - \hat{\mathbf{y}}_{\mathbf{nf}} \tag{5}$$

that quantifies the consistency of the measurement with the model prediction is called a *residual*. We will also call it *observed residual* to distinguish it from *predicted residual* as it will bee seen later. If there is no uncertainty in model (4), the absence of leakage implies $\mathbf{r} = 0$.

In a leakage scenario, only the possibility of one leak of nominal value f^0 in an unknown node of the network is considered. The nominal value of the leak affects equations (2) and (3)

$$q^{in} = \sum_{i=1}^{n_d} d_j + f^0 \tag{6}$$

$$d_i(q^{in} - f^0) = \alpha_i(q^{in} - f^0) \tag{7}$$

Consider the n_d predictions $\hat{\mathbf{y}}_{\mathbf{f_i}}$, each one corresponding to a leak of nominal value f^0 in node i

$$\hat{\mathbf{y}}_{\mathbf{f_i}} = \mathbf{g}_{f_i}(q^{in}, \mathbf{h}_S, \mathbf{d}(q^{in} - f^0), f^0) \qquad i = 1 \dots n_d \tag{8}$$

where $\hat{\mathbf{y}}_{\mathbf{f_i}} \in \Re^{n_y}$, $\mathbf{g}_{f_i} : \Re \times \Re^{n_h} \times \Re^{n_d} \times \Re \to \Re^{n_y}$. Subscript f_i indicates a faulty scenario consisting of a leak in node i. The differences $\hat{\mathbf{r}}_{\mathbf{f_i}} = \hat{\mathbf{y}}_{\mathbf{f_i}} - \hat{\mathbf{y}}_{\mathbf{nf}}$ are the predicted residuals for the nominal leak f^0.

3 Proposed Approach

Given a set of measurements and models that represent different leakage scenarios, the proposed methodology aims to select the model that is more consistent with these measurements. Each scenario considers only one leak in a different location (node) of the network. Therefore, selecting the most consistent scenario is equivalent to selecting the most consistent location for the leak. Different authors have studied the problem of leak location from different perspectives. In [21] a complete mathematical view of the consistency problem as an inverse problem is given. In [18, 23] the point of view of model-based fault diagnosis is taken [3] In all mentioned works, the idea is to solve the consistency problem with algorithms that can use existing efficient network solvers for the forward problem. This work takes the approach described in [24] and it differs from the one in [16, 23] only in the correlation measure. In this approach, a leak in a node will be considered to be a fault that is to be localized. The algorithm gives the most consistent location for a leak given a set of measurements from the network. First, the leak location problem will be tackled for one time step and the time argument will be omitted. Later, the use of information from more than one time steps will be described.

For clarity we first explain how the location would be performed if only measurements from one time step were available. If there is no uncertainty in model (8) and the value of the unknown leak to be located is small enough, then the dependency of the observed residual $\mathbf{r}$ can be supposed to be approximately linear in leak f

$$\mathbf{r} = \hat{\mathbf{r}}_{\mathbf{f_i}} \cdot \frac{f}{f^0} \qquad i = 1 \dots n_d \tag{9}$$

And the residual leak sensitivities collected in the *Fault Sensitivity Matrix* denoted by Ω

$$\Omega = \begin{bmatrix} \frac{\partial r_1}{\partial f_1} & \cdots & \frac{\partial r_1}{\partial f_{n_d}} \\ \vdots & \ddots & \vdots \\ \frac{\partial r_{n_y}}{\partial f_1} & \cdots & \frac{\partial r_{n_y}}{\partial f_{n_d}} \end{bmatrix}. \tag{10}$$

following the ideas in [21], this matrix can be approximated by

$$\Omega \simeq \frac{1}{f^0}[\hat{\mathbf{r}}_{\mathbf{f_1}}, \ldots, \hat{\mathbf{r}}_{\mathbf{f_{n_d}}}] \tag{11}$$

Because of linearity of $\mathbf{r}$ in f, if vectors $\hat{\mathbf{r}}_{\mathbf{f_i}}$ are linearly independent, then each $\hat{\mathbf{r}}_{\mathbf{f_i}}$ characterizes a different leak. Therefore a correlation measure to test linear dependency between $\mathbf{r}$ and $\hat{\mathbf{r}}_{\mathbf{f_i}}$ can be used to select the most consistent leak with $\mathbf{r}$. Thus the selected leak is the one maximizing the correlation measure

$$\rho(\mathbf{r}, \hat{\mathbf{r}}_{\mathbf{f_i}}) = \frac{\mathbf{r}^T \cdot \hat{\mathbf{r}}_{\mathbf{f_i}}}{\| \mathbf{r} \| \| \hat{\mathbf{r}}_{\mathbf{f_i}} \|} \tag{12}$$

where $\| \, . \, \|$ denotes the norm associated to the vector dot product. In this work the 2 norm is used.

Algorithm 2 summarizes the leak location procedure for one time step.

Algorithm 1 Leak location for one time step

Require: q^{in} , $\mathbf{h_S}$, $\mathbf{y}$, $(\alpha_1, \ldots, \alpha_{n_d})^T$, f^0
  $\mathbf{d} = q^{in} (\alpha_1, \ldots, \alpha_{n_d})^T$
  $\hat{\mathbf{y}}_{\mathbf{nf}} = g_{nf}(q^{in}, \mathbf{h_S}, \mathbf{d})$
  $\mathbf{r} = \mathbf{y} - \hat{\mathbf{y}}_{\mathbf{nf}}$ to discard a leakage scenario
  if $\mathbf{r} = 0$ **then**
    return 'No leakage scenario'
  else
    $\mathbf{d} = (q^{in} - f^0) (\alpha_1, \ldots, \alpha_{n_d})^T$
    $\hat{\mathbf{y}}_{\mathbf{f_i}} = g_{f_i}(q^{in}, \mathbf{h_S}, \mathbf{d}, f^0), \quad i = 1 \ldots n_d$
    $\hat{\mathbf{r}}_{\mathbf{f_i}} = \hat{\mathbf{y}}_{\mathbf{f_i}} - \hat{\mathbf{y}}_{\mathbf{nf}}, \quad i = 1 \ldots n_d$
    Select the node index i^* that maximizes $\rho(\mathbf{r}, \hat{\mathbf{r}}_{\mathbf{f_i}})$
  end if
  return i^*

3.1 Using information from more than one time step

As it is described in Section 2, measurements are acquired at sampling time T_s but the localization methodology is applied at a larger time T_L considering the average of the last N_L measurements. Then every time T_L, an average residual $\bar{\mathbf{r}}(kT_L)$ is computed as the difference of the average measurements $\bar{\mathbf{y}}(kT_L)$ and estimations $\bar{\hat{\mathbf{y}}}_{nf}(kT_L)$. In the same way, average predicted residuals $\bar{\hat{\mathbf{r}}}_{\mathbf{f_i}}(kT_L)$ $i = 1, \ldots, n_d$ can be computed.

To improve the characterization of a persistent leak, instead of only $\bar{\mathbf{r}}(kT_L)$ and $\bar{\hat{\mathbf{r}}}_{\mathbf{f_i}}(kT_L)$, the concatenation of these two vector over the last M samples $\bar{\mathbf{r}}((k-M+1)T_L : kT_L)$ and $\bar{\hat{\mathbf{r}}}_{\mathbf{f_i}}((k-M+1)T_L : kT_L)$ are considered, where

$$\bar{\mathbf{r}}((k-M+1)T_L : kT_L) = (\bar{\mathbf{r}}^T((k-M+1)T_L), \ldots, \bar{\mathbf{r}}^T(kT_L))^T$$

$$\bar{\hat{\mathbf{r}}}_{\mathbf{f_i}}((k-M+1)T_L : kT_L) = (\bar{\hat{\mathbf{r}}}_{\mathbf{f_i}}{}^T((k-M+1)T_L), \ldots, \bar{\hat{\mathbf{r}}}_{\mathbf{f_i}}{}^T(kT_L))^T$$

Therefore, the correlation to be maximized to select the most consistent leak at time kT_L considering a past time horizon $H_M = M \cdot T_L$ is

$$\rho(\bar{\mathbf{r}}((k-M+1)T_L : kT_L), \bar{\hat{\mathbf{r}}}_{\mathbf{f_i}}((k-M+1)T_L : kT_L)) \tag{13}$$

Algorithm 2 summarizes the leak location procedure in steady state, i.e. after a time $M \cdot T_L$.

Algorithm 2 Leak location in steady state

Require: $(\alpha_1, \ldots, \alpha_{n_d})^T, f^0$
At each jT_s :
Obtain the sensor values and save in $\mathbf{y}(jT_s), q^{in}(jT_s), \mathbf{h_S}(jT_s)$
Compute $\mathbf{d}(jT_s)$, $\hat{\mathbf{y}}_{\mathbf{nf}}(jT_s)$, $\hat{\mathbf{y}}_{\mathbf{f_i}}(jT_s)$, $\quad i = 1 \ldots n_d$
Compute $\mathbf{r}(jT_s) = \mathbf{y}(jT_s) - \hat{\mathbf{y}}_{\mathbf{nf}}(jT_s)$
Compute $\hat{\mathbf{r}}_{\mathbf{f_i}}(jT_s) = \hat{\mathbf{y}}_{\mathbf{f_i}}(jT_s) - \hat{\mathbf{y}}_{\mathbf{nf}}(jT_s), \quad i = 1 \ldots n_d$
At each kT_L :
Compute the means $\bar{\mathbf{r}}(kT_L)$ and $\bar{\hat{\mathbf{r}}}_{\mathbf{f_i}}(kT_L)$
Construct vectors $\bar{\mathbf{r}}((k-M+1)T_L : kT_L)$ and $\bar{\hat{\mathbf{r}}}_{\mathbf{f_i}}((k-M+1)T_L : kT_L)$
Select the leak $f_I(kT_L)$ that maximizes $\rho(\bar{\mathbf{r}}((k-M+1)T_L : kT_L), \bar{\hat{\mathbf{r}}}_{\mathbf{f_i}}((k-M+1)T_L : kT_L))$, $i = 1 \ldots n_d$
Output $f_I(kT_L)$ to the user

4 Simulations and Results

The leak location methodology presented has been tested in a DMA of Barcelona under a real leak scenario called Nova Icaria, described in Chapter **??**. The Nova Icària DMA has flow and pressure sensors at every inlet, and six inner pressure sensors, whose placement is also marked in Figure 2.

Generally, flow and pressure sensors existing in the DMA networks are integrated with a SCADA system used to supervise these complex systems. The SCADA system monitors the pressure and flow at the inlets of every DMA. This monitoring process is carried out by multi-channel data loggers linked to every inlet which, on the one hand, registers these measurements with a sampling time T_s, of 10 min and on the other hand, is integrated with the SCADA through a GSM (global system mobile for mobile communication) network. Thereby, every day at 7 a.m., the SCADA system retrieves the inlet measurements of all DMAs from 00:00 h to 23:50 h of the previous day. After these data are retrieved, a data validation process fills database with validated data. The inner pressure sensor measurements are required to carry out the leak localization process. These measurements are recorded in a similar way

as DMA inlets. Pressure measurements resolution is 0.1 mwc. The oversampling described in Section 3 is done through the localization period T_L, of 1 h.

To ease the access to the DMA measurements stored in the SCADA validated database, once the DMA measurements of the day before are available, these data are packed in a XLS file and are sent by e-mail to those workstations where the leak localization models are available. Figure 1 shows the conceptual integration between the Nova Icària instrumentation data and the model-based leak localization methodology.

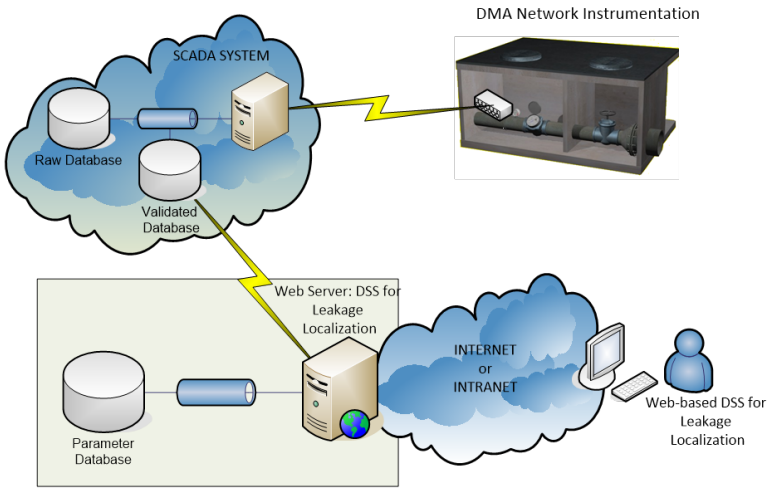

Fig. 1: A conceptual scheme of the decision support system for leak localization highlighting the main processes: online measurements gathered by the district metered area (DMA) instrumentation, data transmission from sensors data loggers to the water company supervisory control and data acquisition system (SCADA), data validation process and validated database population, and leak localization analysis carried out in the leakage localization tool using the DMA EPANET hydraulic model (parameter database).

To assess the leak localization methodology, a leak was forced in the Nova Icària DMA using a discharge component. The experiment took place on December 20, 2012 at 00:30 h and lasted around 30 h; the exact locations exact location of the leak is indicated in Figure 2. The leak effect can be observed in Figure 3(a), where the time evolution of the DMA total inflow on December 20, 2012, affected by the leakage event, and on December 19, 2012, unaffected by the leakage event, has been plotted, showing the significant flow increase caused by the leakage.

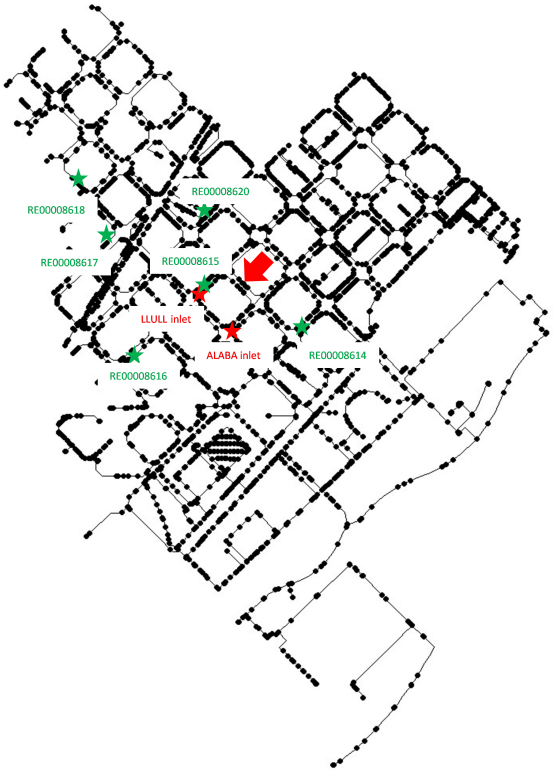

Fig. 2: The water network of Nova Icària district metered area (DMA) (EPANET model) highlighting inner pressure sensors (green stars), DMA inlets (red stars), and the exact location of the leak (red arrow) that was intentionally introduced to test the method.

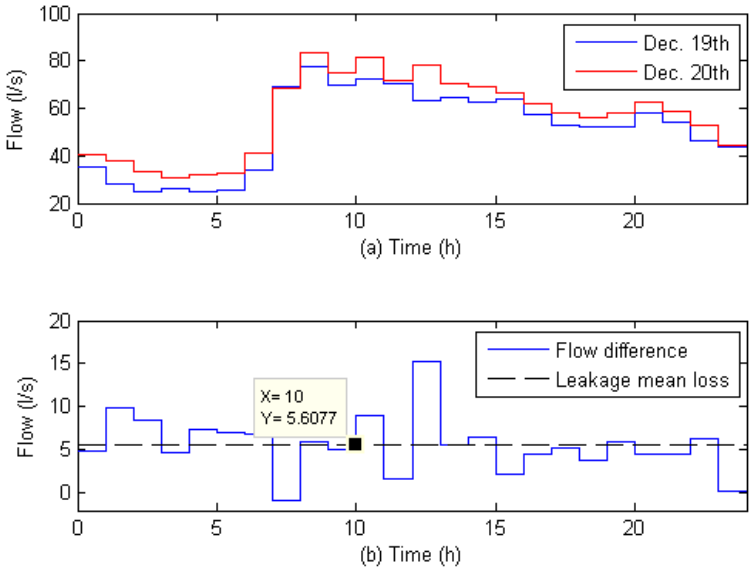

Fig. 3: Leak size estimation: (a) time evolution of the Nova Icària district metered area total inflow on December 20, 2012 affected by the leak event and on December 19, 2012 unaffected by the leak and (b) time evolution of the difference between these two previous flows and its average value (leakage size estimation).

The first stage in the fault diagnosis process is to detect the occurrence of a new leakage scenario in the DMA. In general, a detection procedure followed by water utilities is based on the analysis of the difference between night flows. Although leakage is pressure dependent, and night-time pressure is lower, the fact that at night the demand uncertainty is smaller makes the analysis of night flows more reliable than that of day flows. As shown in Figure 3(a), the total DMA inflow significantly increased on December 20 when the leak occurred compared to the previous day. The difference between these two flows (Figure 3(b)) and the average difference is an estimate of the leak. In this case, the estimated size of the leak is about 5.6 l/s. The model-based leak localization methodology requires the estimation of the emitter coefficient *Ce*, which according to Chapter **??** can be obtained using the estimated average size of the leakage (5.6 l/s, Figure 3(b)) and an estimate of the average pressure at the leak location. This pressure value has been estimated to be about 50 mwc by averaging the measurements of the DMA inner pressure sensors (Figure 4) for December 20. As a result, and using γ =0.5 (the Darcy-Weisbach formula in Chapter **??**), the estimated emitter coefficient is 0.8. The peaks in the leakage observed in Figure 3 are modulated by the network pressure.

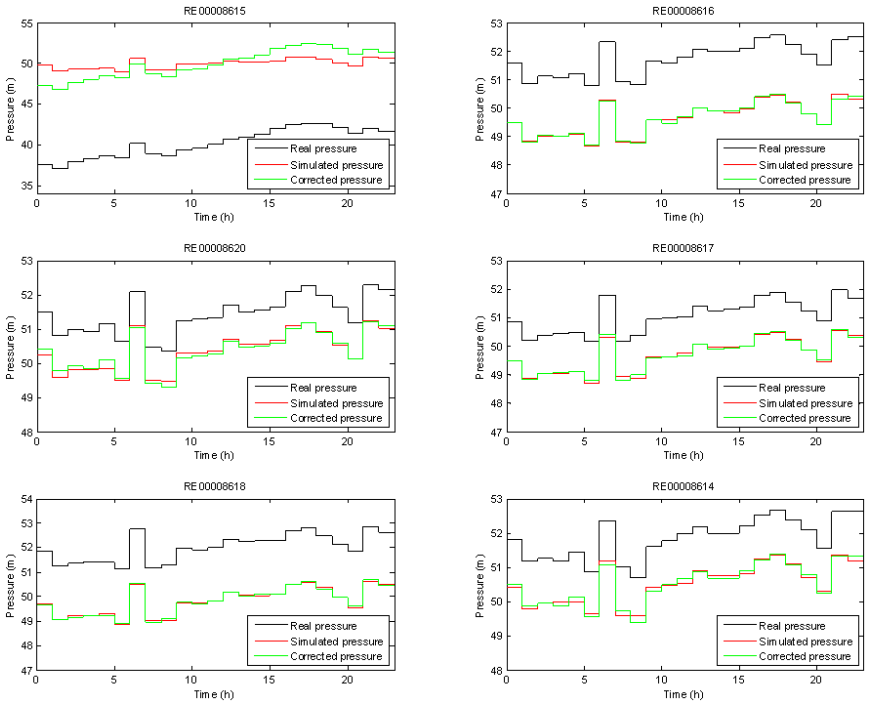

Fig. 4: The time evolution of the measurements of the inner pressure sensors (black), their model simulated values (red), and the corrected measurement values (green). Only sensor RE00008615 shows a different trend and shape when simulated, in comparison to the measurement. Sensor RE00008615 is considered faulty because its mismatch cannot be attributed to bad topographic data, which was confirmed by the operators of the network. Thus, sensor RE00008615 should not be used in further leak localization analyses.

After the detection and size estimation of the leak, the calibration of the DMA hydraulic model and the inner pressure sensors are compared for verification, since existing model errors or poor calibrations may lead to low confidence in the performance of the leak isolation methodology. To carry out the model verification, the data of December 19 have been used since no major leaks were present that day. The general procedure to calibrate the DMA hydraulic model derives from [23] where the pressure in the DMA inlets at time instant k is fixed while the flow value in the inlets at this time instant is distributed among all the DMA inner nodes according to the values of their base demand and related demand patterns. The water demand model described in Chapter **??** is one of the main sources of uncertainty that may lead to inaccurate performance, and, consequently, special attention should be paid in their calibration. In the application considered in this chapter, the base demand of the network nodes has been obtained from the billing information of this DMA by Aigües de Barcelona (Chapter **??**). Each base demand corresponds to the aggregation of consumers attached to a single node, assuring stability in demands.

As an output of the whole model calibration process, a calibrated model of the DMA hydraulic network at every time instant k is obtained, which can be used to predict flow values in the DMA inlets and the pressure in the monitored DMA inner nodes. In Figure 5, the time evolution of the measured and predicted inflows at (a) Alaba and (b) Llull inlets for December 19 is observed, showing the degree of accuracy achieved after the calibration of the hydraulic model. According to the obtained results (Figure 5), certain bounded modeling errors still exist, which may be due to the existing uncertainty in the hydraulic network parameters and the considered demand model [17]. Nonetheless, these inflows are acceptable to obtain a reliable performance of the leak localization methodology.

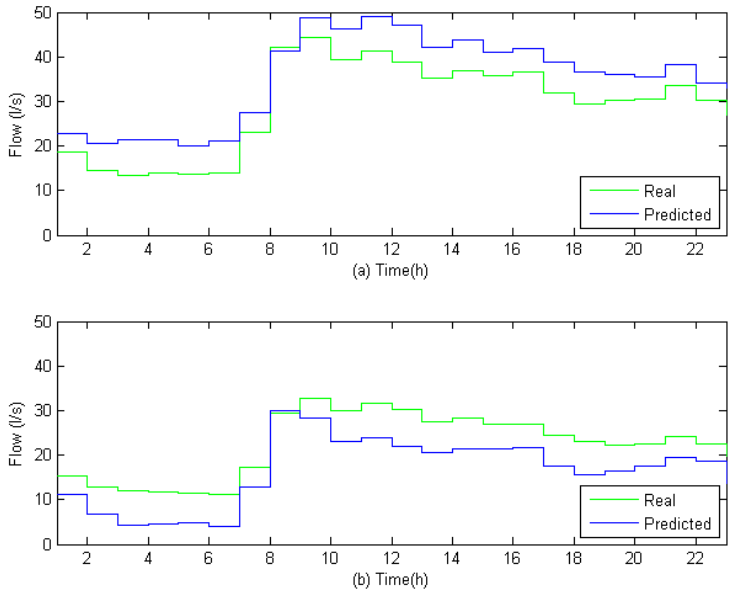

Fig. 5: The time evolution of the measured (green) and predicted (blue) inflows in (a) Alaba and (b) Llull inlets for December 19 showing the degree of accuracy achieved once the hydraulic model has been calibrated.

Regarding the DMA inner pressure sensors, divergence between real measurements and the model simulated values arise, as depicted in Figure 5, due to inaccurate estimation of the depth of the measurement points. Indeed, before carrying out the leakage scenario considered here, the inner pressure sensor RE00008615 presented an abnormal behavior and consequently, was considered unreliable and excluded from the analysis. Thereby, assuming that no major leaks were present on December 19, and that the rest of the pressure sensors were reliable, the dif-

ferences between measured and model-simulated pressures have been adjusted to correct topographic errors in the model. In Figure 4, DMA inner pressure sensor measurements time series, their resulting values after model correction, and the corresponding model predictions have been plotted for December 19. This figure shows that there is a mismatch between the sensor measurements and the predictions given by the model. After estimating the average value of this mismatch for every sensor and correcting the sensor measurements accordingly, the corrected measurements describe the model predictions. The correction factor used to adjust the sensor measurements and the model predictions have been used to update the known, but inaccurate, sensor depths when the leak localization methodology is applied on December 20 to perform leak localisation.

Applying the data analysis described above, the occurrence of leakage on December 20 was detected and the quality of the calibrated DMA hydraulic model was evaluated using sensor measurements from December 19. The leak localization methodology was applied to analyze the sensor data of December 20 to obtain the most probable locations of the detected leak. This methodology has been packaged in a model-driven tool to make it easy to apply to different scenarios [12]. The tool provided an hourly result in the Nova Icària leakage scenario on December 20.

When applying this procedure to obtain the result for a certain hour, it must be taken into account that the used inner pressure sensors have a constrained resolution, as defined previously. This low resolution, together with existing noise in the measurements, may be a source of inaccuracy in the computed results. To overcome the undesired effects derived from the sensor constrained resolution, two main strategies have been considered. First, the sensor measurement considered at a certain hour is the result of applying an average filter to the measured values during the last $T_L = 1$ hour (six times $T_s = 10$ min measurements in (1)). Second, pressure measurements and model predictions from consecutive hours can be accumulated along a cumulative time window of a given length to obtain an accumulated observed residual and an accumulated sensitivity matrix. In the present case, a H_M=10 h-length cumulative window has been used so the observed residuals (r in (5)) and the Sensitivity Matrix (Ω in (10)) from the last 10 h are used to generate the resulting correlation vector (12) at each step, so that those nodes with the highest leak probability can be determined. To analyze the leakage scenario, data from December 20 to December 21 have been used, obtaining a leak correlation vector at each time instant (that is, one per hour).

The value of the jth component determines the correlation between the observed residual and the theoretical fault signature (jth column of the Ω) predicted by the model for a leak placed in the jth node of the network ((11)). The correlation vector can be represented graphically on the top of the DMA using a gray map where the highest correlations are darker than lower correlations. The level of gray depends on the highest correlation obtained at every time instant, which means that the graphical representation associated with a certain time instant cannot be directly compared with the one of another time instant since the associated highest correlation value may be different. In this graphical representation, those nodes with the highest correlation value (c_{max}) are depicted with a black star. Additionally, a cross point to the

center of gravity of the set of nodes with high correlation (in this case, those whose correlation value c is greater than $0.99c_{max}$).

Figure 6 shows four graphical representations of the correlation vector obtained with the leak isolation methodology for December 20 at $T_L = 14$ h (Figure 6a), $T_L = 15$ h (Figure 6b), and $T_L = 22$ h (Figure 6c), when the leak is still present; and December 21 at $T_L = 20$ h ((Figure 6d), when the leak is already fixed. Thus, Figures 6a, b and c signal a potential leak moving around a little zone of the network with correlations oscillating between 0.6 and 0.75 (maximum correlation value is one). Figure 6d depicts the correlation vector after the leak is fixed, pointing out the meaningful decrease of the resulting highest correlation value regarding the cases when the leakage is still present.

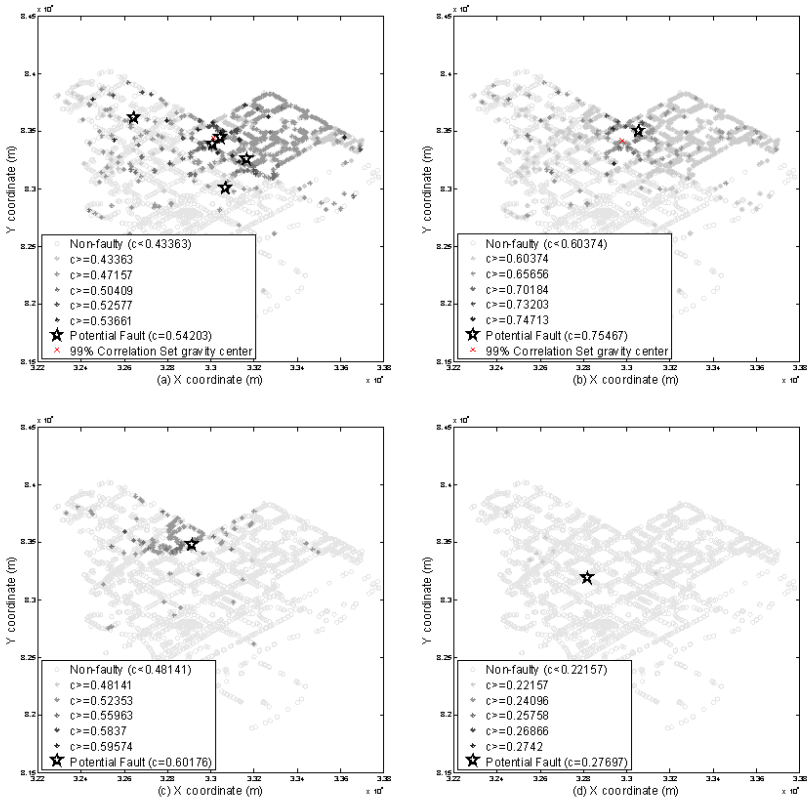

Fig. 6: Correlation vector obtained with the leak isolation methodology for December 20 at (a) $T_L = 14$ h, (b) $T_L = 15$ h, (c) $T_L = 22$ h and and December 21 at (d) $T_L = 20$ h

In Figure 7, the resulting correlation vectors obtained at every time instant during December 20 and 21 have been accumulated to determine the nodes with the highest

correlation. Consequently, the most probable leak locations according to this 48-h time window are determined (only those correlation values higher than 0.5 are considered). The star size depends on the resulting value of the accumulated correlation. The bigger the star is, the bigger the corresponding accumulated correlations. Additionally, in Figure 7 the real location of the leak has also been signaled using a red star and that area containing the nodes with the higher accumulated correlation values has been marked using an ellipsoid with a red outline. Comparing the leak localization indications given by the method to the real location of the leak, the resulting error is considered acceptable in the sense that the predicted area of the leak has an acceptable size containing the real location of the leak. It must be considered that the resulting error is mainly due to the inconsistency between the hydraulic and demand models and the sensor measurements. Note that a nodal leak localization using a small set of sensors determines potential network areas where the leak is located, rather than the exact node where the leak is. This situation occurs because, when using few sensors, there could be certain leaks causing the same pressure disturbance from the point of view of the used sensor network and consequently, isolation among the potential leaks cannot be carried out.

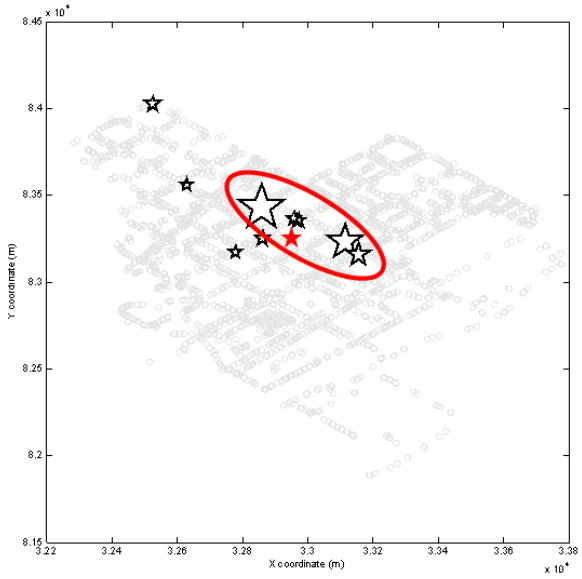

Fig. 7: A graphical representation (black stars) of the most probable localizations of the leak according to the accumulation of the resulting correlation vectors related to every node through a 48-h time window (December 20 and 21): the bigger the star size, the bigger are the corresponding accumulated correlations. Additionally, the real location of the leak (red star) and the area containing those nodes with the highest correlations values (red outline ellipsoid) are also shown.

5 Conclusions and Research Prerspectives

This chapter presents a model-based methodology for leak localization in WDNs using pressure measurements. The method presented uses residuals obtained from the pressure measurements and their estimates from the network hydraulic model that characterizes the behavior of the DMA without leakage. The residuals are compared with the Fault sensitivity Matrix that contains the predicted pressure disturbance caused by each potential leak in all of the monitored networks inner nodes (theoretical fault sensitivity). Leak isolation relies on correlating the observed residuals with the theoretical fault sensitivity contained in the Fault Sensitivity Matrix. The leak localization methodology has been implemented in a software tool that interfaces with a geographic information system and allows the easy use by water network manager. Simulation results obtained applying the method to a DMA of the Barcelona WDN highlight the effectiveness of the approach. Finally, a real application of this method on the Nova Icària DMA pilot test has been presented showing satisfactory results in a real fault scenario.

Regarding future research related to this subject, several issues remain open. One research issue is to quantify the effect of uncertainties in demands, sensors, and leak magnitude estimation on the methodology and accuracy of the leak localization procedure. Another related issue is to reduce the impact of uncertainty on the detection and isolation process. It is also of interest to extend the methodology to the detection and isolation of multiple leaks, and to complement the methodology with a sensor-fault detection process, to guarantee that only valid sensor data are used for leak detection.

References

1. ADEC. Technical Review of Leak Detection Technologies - vol.1 - Crude Oil Transmission Pipelines. Technical report, Alaskan Department of Environmental Conservation, Alaska, 2000.
2. The World Bank. Reducing Water Loss in Developing Countries Using Performance-Based Service Contracting 44722. *P-notes*, 2006(4):2006–2009, 2008.
3. M. Staroswiecki. Blanke, M. Kinnaert, J. Lunze. *Diagnosis and Fault-tolerant Control*. Springer, Berlin, 2 edition edition, 2006.
4. Andrew F. Colombo, Pedro Lee, and Bryan W. Karney. A selective literature review of transient-based leak detection methods. *Journal of Hydro-environment Research*, (4):212–227, April.
5. Ben Farley, Stephen R. Mounce, and Joby B. Boxall. Field Validation of "Optimal" Instrumentation Methodology for Burst/Leak Detection and Location. In *Water Distribution Systems Analysis 2010*, pages 1093–1102, Reston, VA, December. American Society of Civil Engineers.
6. James-A. Goulet, Sylvain Coutu, and Ian F.C. Smith. Model falsification diagnosis and sensor placement for leak detection in pressurized pipe networks. *Advanced Engineering Informatics*, (2):261–269, April.
7. Jean-Marie Henault, Gautier Moreau, Sylvain Blairon, Jean Salin, Jean-Robert Courivaud, Frédéric Taillade, Erick Merliot, Jean-Philippe Dubois, Johan Bertrand, Stéphane Buschaert,

Stefan Mayer, and Sylvie Delepine-Lesoille. Truly Distributed Optical Fiber Sensors for Structural Health Monitoring: From the Telecommunication Optical Fiber Drawling Tower to Water Leakage Detection in Dikes and Concrete Structure Strain Monitoring. *Advances in Civil Engineering*, pages 1–13.

8. J. Hugenschmidt and A. Kalogeropoulos. The inspection of retaining walls using GPR. *Journal of Applied Geophysics*, (4):335–344, April.
9. Zoran Kapelan, Dragan Savic, Godfrey Walters, D. Covas, I. Graham, and C. Maksimovic. An assessment of the application of inverse transient analysis for leak detection: Part I. In *International Conference on Advances in Water Supply Management*, London, 2003.
10. Sang Hyun Kim. Extensive Development of Leak Detection Algorithm by Impulse Response Method. *Journal of Hydraulic Engineering*, (3):201–208, March.
11. James Liggett and Li Chen. Inverse Transient Analysis in Pipe Networks. *Journal of Hydraulic Engineering*, (8):934–955, August.
12. Jordi Meseguer, Josep M Mirats-tur, Gabriela Cembrano, Vicenç Puig, Gerard Sanz, David Ibarra, and Joseba Quevedo. Environmental Modelling & Software A decision support system for on-line leakage localization n P e. 60:331–345, 2014.
13. S. R. Mounce, J. B. Boxall, and J. Machell. Development and Verification of an Online Artificial Intelligence System for Detection of Bursts and Other Abnormal Flows. *Journal of Water Resources Planning and Management*, (3):309–318, May.
14. Stephen R. Mounce, Richard B. Mounce, and Joby B. Boxall. Novelty detection for time series data analysis in water distribution systems using support vector machines. *Journal of Hydroinformatics*, (4):672, October.
15. C. V. Palau, F. J. Arregui, and M. Carlos. Burst Detection in Water Networks Using Principal Component Analysis. *Journal of Water Resources Planning and Management*, (1):47–54, January.
16. R. Pérez, M.-A. Cugueró, J. Cugueró, and G. Sanz. Accuracy Assessment of Leak Localisation Method Depending on Available Measurements. *Procedia Engineering*, pages 1304–1313.
17. Ramon Pérez, Fatiha Nejjari, Vicenç Puig, Joseba Quevedo, Gerard Sanz, Miquel Cugueró, and Antoni Peralta. Study of the isolability of leaks in a network depending on calibration of demands. In *11th International Conference on Computing and Control for the Water Industry*, pages 455–460, Exeter, 2011.
18. Ramon Pérez, Vicenç Puig, Josep Pascual, Joseba Quevedo, Edson Landeros, and Antonio Peralta. Methodology for leakage isolation using pressure sensitivity analysis in water distribution networks. *Control Engineering Practice*, (10):1157–1167, October.
19. Ramon Pérez, Gerard Sanz, Vicenc Puig, Joseba Quevedo, Miquel Angel Cuguero Escofet, Fatiha Nejjari, Jordi Meseguer, Gabriela Cembrano, Josep M. Mirats Tur, and Ramon Sarrate. Leak Localization in Water Networks: A Model-Based Methodology Using Pressure Sensors Applied to a Real Network in Barcelona [Applications of Control]. *IEEE Control Systems*, (4):24–36, August.
20. R. Pilcher. Leak location and repair guidance notes and... the never ending war against leakage. In *Water Loss 2*, 2007.
21. Ranko Pudar and James Liggett. Leaks in Pipe Networks. *Journal of Hydraulic Engineering*, (7):1031–1046, July.
22. R. Puust, Z. Kapelan, D. a. Savic, and T. Koppel. A review of methods for leakage management in pipe networks. *Urban Water Journal*, (1):25–45, February.
23. Joseba Quevedo, Miquel Cugueró, Ramon Pérez, Fatiha Nejjari, Vicenç Puig, and Josep Mirats. Leakage Location in Water Distribution Networks based on Correlation Measurement of Pressure Sensors. In *8th IWA Symposium on Systems Analysis and Integrated Assessment*, pages 290–297, San Sebastián, 2011. IWA.
24. Gerard Sanz Ramon Pérez, Miquel-Angel Cugueró, Josep Cugueró. Accuracy Assessment of Leak Localisation Method depending on available measurements. In *CCWI2013*, Perugia, 2013.
25. Michele Romano, Zoran Kapelan, and Dragan A. Savić. Automated Detection of Pipe Bursts and Other Events in Water Distribution Systems. *Journal of Water Resources Planning and Management*, (4):457–467, April.

26. Michele Romano, Zoran Kapelan, and Dragan A. Savić. Geostatistical techniques for approximate location of pipe burst events in water distribution systems. *Journal of Hydroinformatics*, 15:634–651, 2013.
27. Gerard Sanz, Ramon Perez, Zoran Kapelan, and Dragan Savic. Leak Detection and Localization through Demand Components Calibration- ACCEPTED. *Journal of Water Resources Planning and Management*, 2015.
28. Derya Sumer and Kevin Lansey. Effect of Uncertainty on Water Distribution System Model Design Decisions. *Journal of Water Resources Planning and Management*, (1):38–47, January.
29. John Vítkovský, Angus Simpson, and Martin Lambert. Leak Detection and Calibration Using Transients and Genetic Algorithms. *Journal of Water Resources Planning and Management*, (4):262–265, July.
30. Zheng Wu and Paul Sage. Water Loss Detection Via Genetic Algorithm Optimization-Based Model Calibration. In *ASCE 8th International Symposium on Water Distribution System Analysis*, Cincinnati, 2006.